Published in final edited form as:

Anal Chem. 2016 January 19; 88(2): 1230–1237. doi:10.1021/acs.analchem.5b03541.

Microfabrication and In Vivo Performance of a Microdialysis Probe with Embedded Membrane

Woonghee Lee[1,a], **Thitaphat Ngernsutivorakul**[1,a], **Omar S. Mabrouk**[a], **Jenny-Marie T. Wong**[a], **Colleen E. Dugan**[a], **Samuel S. Pappas**[b], **Hyeun Joong Yoon**[3,c], and **Robert T. Kennedy**[a]

[a]Department of Chemistry, University of Michigan, 930 N. University Ave, Ann Arbor, MI 48109-1033

[b]Department of Neurology, University of Michigan, 1500 E Medical Center Dr, Ann Arbor, MI 48109-5316

[c]Department of Chemical Engineering, University of Michigan, 2300 Hayward Street, Ann Arbor, MI 48109-2136

Abstract

Microdialysis sampling is an essential tool for in vivo neurochemical monitoring. Conventional dialysis probes are over 220 μm in diameter and have limited flexibility in design because they are made by assembly using preformed membranes. The probe size constrains spatial resolution and governs the amount of tissue damaged caused by probe insertion. To overcome these limitations, we have developed a method to microfabricate probes in Si that are 45 μm thick × 180 μm wide. The probes contain a buried, U-shaped channel that is 30 μm deep × 60 μm wide and terminates in ports for external connection. A 4 mm length of the probe is covered with a 5 μm thick nanoporous membrane. The membrane was microfabricated by deep reactive ion etching through a porous aluminum oxide layer. The microfabricated probe has cross-sectional area that is 79% less than that of the smallest conventional microdialysis probes. The probes yield 2–7% relative recovery at 100 nL/min perfusion rate for a variety of small molecules. The probe was successfully tested in vivo by sampling from the striatum of live rats. Fractions were collected at 20 min intervals (2 μL) before and after an intraperitoneal injection of 5 mg/ kg amphetamine. Analysis of fractions by liquid chromatography-mass spectrometry revealed reliable detection of 13 neurochemicals, including dopamine and acetylcholine, at basal conditions. Amphetamine evoked a 43-fold rise in dopamine, a result nearly identical to a conventional dialysis probe in the same animal. The microfabricated probes have potential for sampling with higher spatial resolution and less tissue disruption than conventional probes. It may also be possible to add functionality to the probes by integrating other components, such as electrodes, optics, and additional channels.

Correspondence to: Robert T. Kennedy.

[1]These two authors contributed equally to this work

[3]Current address is Department of Electrical Engineering and Computer Science, South Dakota State University

INTRODUCTION

Microdialysis is widely used for in vivo sampling. In this technique, a semi-permeable membrane probe is inserted into tissue or fluid and perfused with an isotonic solution. Chemicals in the tissue diffuse across the membrane according to their concentration gradient and are collected in fractions for analysis.[1–3] The popularity of microdialysis stems from its favorable properties. Samples are continuously removed from a well-defined space without net fluid loss from the tissue. The membrane prevents large molecules and debris from being collected that might interfere with downstream assays. Collection of a series of fractions allows changes in tissue chemistry to be monitored over time. The probe can also be used for local delivery of chemicals. Microdialysis is versatile because it can be used to sample from organs, tissues, tumors, and body fluids.[4–8]

Despite the advantages, the size of microdialysis probes creates some limitations. Probes are generally made by coupling capillaries to preformed dialysis tubing resulting in a cylindrical shape with a diameter defined by the dialysis tubing, typically no smaller than 220 μm. The relatively large probe diameter prevents sampling from microenvironments such as small brain nuclei. This problem is especially acute in smaller subjects, like mice, which are often preferred for research because of the extensive genetic tools and models available. Tissue damage with potentially confounding effects on measured chemicals is another issue that is likely worse with larger diameter probes.[9] Finally, in clinical applications, smaller probes are desirable to minimize discomfort and increase precision.[10]

A route to miniaturizing microdialysis probes is by microfabrication. Microfabricated needles without membranes have been applied for drug delivery[11–14] and sampling.[15–18] We have reported a 70 μm wide by 85 μm thick microfabricated “push-pull” probe for in vivo sampling.[19] Sampling occurred by pulling fluid through one channel while pushing an equal volume out the other at 50 nL/min. A limitation of push-pull and needle-type sampling is that proteins and debris can enter the sampling channel potentially interfering with assays or clogging channels. Another issue is that pull-flow connections must be made at the probe. The pull connection complicates sample collection, especially at the low sampling rates used. This plumbing requirement is in contrast to microdialysis where fluids are pumped into the inlet leaving the outlet free for sample collection. Finally, the push and pull flows must be balanced to avoid net fluid loss or gain around the probe. Fluid balancing is challenging at such low flow rates but is not necessary in microdialysis.

A key challenge in microfabricating a microdialysis probe is forming a membrane over an open channel. A variety of semi-permeable membranes have been formed as part of microfluidic systems (see Table S-1 for summary).[10,20–30] Most of these membranes were designed for on-chip sample processing and only a few have been designed as implantable probes. In one example, a cellulose membrane was cast over a parylene channel; however, this probe was actually larger than a conventional dialysis probe and was not demonstrated for sampling.[20] Microdialysis probes have also been fabricated in Si with permeable polysilicon or fabricated pores as the permeable layer.[10,22,23] The polysilicon membrane was too fragile to use with pressure-driven fluid flows in microchannels. Probes with fabricated pores showed excellent promise in vitro although low pore density may limit recovery.

These pioneering designs suggest the potential for in vivo microscale sampling; however, microfabricated dialysis probes with high pore density and suitable recovery have yet to be demonstrated for in vivo sampling.

We have developed a procedure to microfabricate a microdialysis probe in Si. The membrane is formed by electrochemical etching of a porous anodic aluminum oxide (AAO) layer to yield a high density of straight pores with controllable size.[31–33] The porous AAO is used as a mask for deep reactive ion etching (DRIE) of a polysilicon layer that is underneath the AAO and over a microfluidic channel. Utility of the probes was demonstrated by monitoring neurotransmitters in the brain of live animals.

EXPERIMENTAL SECTION

Chemicals and materials

Unless specified otherwise, all chemicals were purchased from Sigma Aldrich (St. Louis, MO) or Fisher Scientific (Fairlawn, NJ) and were certified ACS grade or better. Solutions were prepared with HPLC-grade water or water purified by a Milli-Q system (Millipore, MA). Fused silica capillaries were purchased from Molex (Phoenix, AZ). Epoxy glues were purchased from ITW Devcon (Danvers, MA) and Loctite (Westlake, OH). Crystalbond Adhesive was purchased from Structure Probe (West Chester, PA). Artificial cerebrospinal fluid (aCSF) consisted of 145 mM NaCl, 2.68 mM KCl, 1.10 mM $MgSO_4$, 1.22 mM $CaCl_2$, 0.50 mM NaH_2PO_4, and 1.55 mM Na_2HPO_4, adjusted pH to 7.4 with 0.1 M NaOH. Unions for 360 μm outer diameter (OD) capillaries were purchased from Idex Health and Science (P-772, Oak Harbor, WA).

Microfabrication of microdialysis probe with embedded nanoporous membrane

Overview—The scheme for microdialysis probes was designed in L-EDIT software (Tanner EDA). All processing was performed at the Lurie Nanofabrication Laboratory at the University of Michigan. The overall probe layout is shown in Figure 1. Probes were 11 mm long × 45 μm thick with a shank that narrowed to 160 μm wide at the tip. A microchannel with semicircular cross-section (60 × 30 μm) ran the length of the probe to form an inlet and outlet was fabricated in the surface (Figure 1A). A 4 mm length of the probe at the tip was made porous by DRIE though an electrochemically etched AAO membrane (Figure 1B) that was overlaid the thin Si layer shown in Figure 1A.

Channel formation—Probes were fabricated on 4 inch p-type wafers (Silicon Valley Microelectronics, Santa Clara, CA) using the process outlined in Figure 2. A 2 μm silicon dioxide layer was grown on a wafer by wet oxidation using a Tempress TS 6604 S3 tool. The initial line for channel etching was patterned by lithography in 3 μm of SPR220 photoresist (Dow, Marlborough, MA), see Figure 2A. The exposed SiO_2 was removed with DRIE using the Bosch process (which uses C_4F_8 as a passivation material) with a STS Deep Silicon Etcher (Figure 2A) and semicircular shaped channels (Figure 2B) were formed using a SPTS Xactix XeF_2 etcher (Allentown, PA). Channels were sealed by chemical vapor deposition (Tempress TS 6604 S3/T3) of 3 μm of polysilicon. The polysilicon layer on the wafer surface was etched with DRIE until the buried SiO_2 layer was exposed and then

removed by treatment with buffered hydrofluoric acid (Transene Co Inc, Danvers, MA) for 20 min. An additional 2 μm polysilicon layer was deposited followed by the deposition of a 1 μm SiO_2 layer for recovery of potential damage during the polysilicon removal process (Figure 2C). The probe shape was patterned by a second lithography step and exposed SiO_2 was removed by DRIE. After photoresist removal in PRS 2000 (Avantor Performance Materials, Phillipsburgh, NJ), a sampling area at the probe tip was patterned by a third lithography step. The outline of the probe was etched by DRIE to 150 μm depth and SiO_2 layer on the channel was removed in buffered hydrofluoric acid (Figure 2D). Finally, polysilicon thickness on the sampling area was reduced to 2 μm by DRIE (Figure 2E).

Membrane formation and probe release from wafer—A 400 nm Al layer was deposited over the wafer using an e-beam evaporator (Denton Vacuum, Moorestown, NJ), Figure 2F. The Al coating was anodized at 60 V and 15 °C in 0.3 M oxalic acid solution for 15 min using Pt mesh (Alfa Aesar, Ward Hill, MA) as a counter electrode (see Figure S-1).

The wafer was rinsed with DI water and then treated with 5% phosphoric acid at room temperature for 50 min to widen the pores (Figure 2F). The polysilicon layer overlying the microchannel was etched by DRIE at −15°C using the AAO layer as a mask (Figure 2G). The AAO membrane was removed by treating with 5% phosphoric acid at 65 °C for 1 h (Figure 2H). A fresh 3 μm Al layer was deposited using the Enerjet evaporator. (For this step, the wafer was tilted to a 45° angle in order to prevent blocking of previous etched holes on polysilicon layer by Al metal vapor.) The Al layer was anodized at 60 V and 15 °C in 0.3 M oxalic acid solution for 45 min and pores widened by treating with 5% phosphoric acid at room temperature for 90 min (Figure 2I). The results of each process were imaged by scanning electron microscopy (Hitachi SU8000 SEM). The wafer with embedded AAO membrane was bonded to a carrier wafer with Crystalbond 555 (Structure Probe, Inc., West Chester, PA) and backside etched by DRIE until the probe thickness reached 40 μm (Figure 2J). Individual probes were released in hot water.

Probe holder fabrication and assembly—Resulting probes were too small and fragile to be conveniently handled and plumbed to connection tubing; therefore, a holder was microfabricated similar to that described previously for push-pull probes.[19] Full description of holder fabrication and assembly is given in Figure S-2. 12 cm lengths of 100 μm I.D. × 360 μm O.D. capillary were connected to the inlet and outlet. The outlet capillary was then joined to a 22 cm long, 50 μm I.D. × 360 μm O.D. fused-silica capillary for fraction collection. Flow through probes was driven using a Chemyx syringe pump (Stafford, TX).

In vitro characterization

To determine the dynamic response during sampling, probes were perfused with water at a flow rate of 100 nL/min and placed into a stirred vial of water (see Figure S-3A). The solution was subsequently changed to a 50 μM fluorescein solution while recording fluorescence within the exit tubing using a fluorescence microscope.

For study of probe relative recovery, the microfabricated probe (“μFab”) was compared to a concentric microdialysis probe (“MD”) which was prepared as previously described.[34] The concentric probe had a regenerated cellulose membrane with 18 kDa molecular weight cut-

off that was 4 mm long and 220 μm diameter (Spectrum Labs, Rancho Dominguez, CA). Probes were dipped into a well-stirred vial containing: 0.5 μM acetylcholine (ACh), dopamine (DA), 3-methoxytyramine (3-MT), and serotonin (5-HT); 1 μM 3,4-dihydroxyphenylalanine (DOPA) and histamine (Hist); 10 μM 3,4-dihydroxyphenylacetic acid (DOPAC), γ-aminobutyric acid (GABA), 5-hydroxyindoleacetic acid (5-HIAA), homovanillic acid (HVA), phenylalanine (Phe), and tyrosine (Tyr); 50 μM choline (Cho), serine (Ser), and taurine (Tau); and 1 mM glucose (Gluc) in aCSF at 37 C. The aCSF was supplemented with 0.25 mM ascorbate to protect against oxidation of analytes. After an equilibration time of 30 min, dialysates were collected in 20 min fractions with a perfusion rate of 100 nL/min.

Dialysate samples were derivatized with benzoyl chloride and analyzed by LC-MS, as described previously.[35] Briefly, 1.5 μL of standards or fractions were mixed with 3 μL of 100 mM sodium carbonate buffer at pH 11 and 3 μL benzoyl chloride (2% in acetonitrile, v/v). The samples were mixed with 3 μL of [^{13}C]-labeled or [d4]-labeled benzoylated internal standards, consisting of 5 nM [^{13}C]-DA, [^{13}C]-3-MT, [^{13}C]-5-HT, and [^{13}C]-DOPA; 10 nM [d4]-ACh and [d4]-Cho; 50 nM [^{13}C]-GABA and [^{13}C]-Hist; 125 nM [^{13}C]-DOPAC, [^{13}C]-5-HIAA, and [^{13}C]-Tyr; 0.5 μM [^{13}C]-Tau ad Gln; 1.25 μM [^{13}C]-Phe and [^{13}C]-Ser; and 12.5 μM [^{13}C]-Gluc in 50% acetonitrile v/v containing 1% sulfuric acid. Samples were analyzed using an Accela UHPLC interfaced to a TSQ Quantum Ultra triple quadrupole mass spectrometer (Thermo Fisher Waltham, MA) operated in multiple reaction monitoring mode. 3 μL samples were injected onto a 2.1 mm × 100 mm Phenomenex biphenyl Kinetex HPLC column (Torrance, CA). Mobile phase A was 10 mM ammonium formate with 0.15% formic acid, and mobile phase B was acetonitrile. The mobile phase gradient was: initial, 0% B; 0.01 min, 19% B; 1 min, 26% B; 1.5 min, 75% B; 2.5 min, 100% B; 3 min, 100% B; 3.1 min, 5% B; and 3.5 min, 5% B at 0.45 mL/min.

In vivo sampling

All procedures were conducted according to a protocol approved by the University Committee for the Use and Care of Animals (UCUCA). Male Sprague-Dawley rats weighing between 250–300 g, (Harlan, Indianapolis, IN, USA) were used for all experiments. Rats were housed in a temperature and humidity controlled room with 12 h light/dark cycles with access to food and water *ad libitum*. Measures were taken to prevent animal pain and discomfort throughout the experiment. All animal experiments were within the guidelines of Animal Research Reporting *in vivo* Experiments (ARRIVE).

Animals were anesthetized using 2–4% isoflurane and placed in a stereotaxic frame (David Kopf, Tujunga, CA). Two burr holes were drilled above the striatum +1.0 mm anterior-posterior and ± 3.0 mm lateral from bregma. The MD probe and μFab probe were lowered into opposite hemispheres–6.15 mm from the top of the skull. Rats were maintained under anesthesia for the duration of the experiment using isoflurane. Both probes were perfused with aCSF at 100 nL/min. After 1 h equilibration, two 20 min fractions were collected for basal concentrations (2 μL per fraction) and two more were collected after an amphetamine injection (5 mg/ kg, i.p). Following the experiment, the probes were withdrawn from the

brain using the stereotaxic frame and the rat was euthanized. Brains were extracted to confirm probe placement.

RESULTS AND DISCUSSION

Probes

A challenge in fabricating microdialysis probes is embedding nanoporous membranes over channels while balancing the need for sufficient physical strength and good recovery across the membrane. The process described in Figure 2 allowed formation of a nanoporous membrane covering a total of 8 mm length of channel (but only 4 mm length of probe because the channel has a 180° turn at the tip). The resulting 5 μm thick membrane has straight pores that are 60–80 nm wide at a density of $8.4 \pm 0.2 \times 10^{13}/m^2$ (n = 3), as shown in Figure 3. 50–70 probes (representing a 50% success rate) could be recovered from a single wafer. AAO membranes have been previously used as a photomask on a solid surface;[36] however, our approach is unique in using AAO as a DRIE mask directly over a microchannel.

In preliminary experiments fabrication stopped at step G in figure 2; however, we found that the resulting membranes were fragile and ruptured when attempting to flow through the probe. The additional 3 μm AAO membrane (Figure 2 I-J) gave the probes sufficient mechanical strength. A drawback of this approach is that the final AAO pores do not necessarily line up with the polysilicon pores; however, the pore density was sufficient to give enough overlap and allow molecular exchange as described below.

In vitro characterization

The response of the μFab probe to a change in concentration was determined by switching the sampled solution from 0 μM to 50 μM fluorescein while monitoring fluorescence at the probe outlet (see Figure S3). Fluorescence signals began to increase 14.5 min after switching. This delay is expected because the perfusion rate was 100 nL/min and the internal volume from sampling tip to detection point was ~ 1400 nL. The good agreement shows that leakage through the system was insignificant and allows accurate correlation of concentration changes in collected fractions and time of event in the sample. Once the fluorescence signal increased, it had a 10 – 90% rise time of 47 ± 2 s (n = 7). This rise time, which determines the best possible temporal resolution, is close to the estimated rise time of 44 s using the combined diffusion and Taylor dispersion equation.[37] The predicted rise time is 1 s for probe channel and 43 s for combined outlet and collection capillaries. Because most of the dispersion is in the connecting channel, it may be possible to improve temporal resolution by using segmented flow or smaller connection capillaries.[37–39]

In vitro relative recovery of neurochemicals was evaluated by comparing dialysate samples with samples taken directly from the stirred vial (Table S-2). For the μFab probe, the recovery was from 2 to 7% for selected neurochemicals. The variation in recovery may be caused by differences in molecular structure, charge effects, hydrophobicity, and membrane specificity. These results can be contrasted with the nearly 100% relative recovery obtained using the traditional probe at 100 nL/min. Compared to the MD probe, the μFab probe

provides lower relative recovery values, at least in part, because of its 6-fold smaller surface area of sampling.

To gain more insight into the recovery, computational simulation of fluid flowing through the μFab probe was performed (see Figure S-4). Initial modeling indicated that flow rate and membrane porosity are the main variables that significantly affect recovery. Using the diffusion coefficient for dopamine,[40] estimated porosity of 33% and flow rate of 100 nL/min (Figure S-4 A), the simulated recovery was 98%, much larger than our observed value of 5 – 7% for dopamine. When porosity was lowered to 1%, the simulated and actual recovery matched (Figure S-4 B). These results suggest that porosity is lower than expected. This discrepancy may be due to several factors. The final overlaid AAO pores do not line up with the polysilicon pores resulting in lower porosity than measured by observing the top of the membrane surface. Some pores may also be clogged, e.g., with wax (used for wafer-mounting) during back-side etching. Changes in probe processing or modifying surfaces may prove useful to improve recovery.[41,42]

In vivo sampling

To determine their suitability for *in vivo* experiments, μFab probes were used to sample from the striatum of anesthetized rats. 13 neurochemicals were consistently detected in 20 min fractions with good signal to noise ratio (Figure 4B). For comparison, we also sampled from the same animals with a MD probe operated at the same flow rate. Basal concentrations from both types of probes are reported in Table 1. Concentrations were not corrected for recovery; however, the MD probes achieved nearly 100% recovery and therefore these concentrations can be considered a good estimate of the in vivo concentration[11]. Comparison of these concentrations with other reports of calibrated in vivo MD experiments reveals reasonable agreement for most neurochemicals.[39,43–49] Acetylcholine and dopamine are generally found in low nanomolar concentrations. Phenylalanine, 5-HIAA, and tyrosine are typically in low micromolar range (< 10 μM) while glutamine, serine and taurine are in high micromolar range (> 10 μM). We observed about 5 times higher concentration of glucose than prior reports; however, our experiment was performed with anesthetized rats which may account for this difference.

Because the MD probe recovery approaches 100% at 100 nL/min, the in vivo recovery of μFab probe could be estimated by dividing dialysate concentrations from μFab probes by dialysate concentrations from MD probes. This calculation assumes that the in vivo concentration is the same on both sides of the brain and at both probes. As shown in Figure 4, the in vitro recovery and estimated in vivo recovery of the μFab probe are comparable for 7 of the neurochemicals. For several compounds (Gln, HVA, Tyr, Ach, DOPAC, and Ser) the estimated in vivo recovery is significantly higher than in vitro recovery. The origin for this difference is not clear. It is possible that active processes and mass transport within the brain is sufficiently different from in vitro for these analytes to cause the in vitro recovery to differ from the in vivo recovery.[50,51] Another interpretation is that the actual basal concentrations from the sampling site of μFab probe are higher than the concentrations from MD probe sampling. Such discrepancies could be due to differences in local concentrations (different

areas were sampled) or to artifacts that result from different tissue reactions due to membrane material and probe size.

To assess the probe performance in response to dynamic in vivo chemical changes, the μFab and MD probes were simultaneously used to monitor concentration changes of DA and other neurochemicals after AMPH administration. When expressing the changes as a percent of baseline, nearly identical changes are seen at both the MD and μFab probes as shown in Figure 5. The large change of about 4300% for DA is in agreement with expected effect of AMPH which inhibits uptake and promotes secretion of DA.[52] Other measured neurochemicals that have significant changes ($p < 0.05$, Student's t-test) in their post drug levels were DOPAC, DOPA, HVA, 5-HIAA, and Tyr. The overall results show the μFab probe provides dynamic measurements nearly the same to a MD probe under the conditions of 100 nL/min flow rate and 20 min fractions.

Histological examination of the sampling sites from both types of probes were performed to visualize overall probe placement within the brain (see Figure S-5). The μFab probe generates a much smaller tract than the MD probe as expected. This difference presumably results in lower tissue damage.

CONCLUSIONS

The in vivo results show that the μFab probe can be reliably used for studying neurochemicals and monitoring dynamic chemical changes in live animal brain. The chief advantage of the probes is that they have 79% smaller cross-section than conventional MD probes and therefore can be used in smaller subjects and brain regions. Despite the small size, the probes are strong enough to penetrate tissue without flexing or breaking. The low recovery at 100 nL/min is a drawback of these probes; however, preliminary experiments suggest that small changes membrane fabrication will mitigate this issue. Fortunately, the excellent sensitivity of LC-MS allows many neurochemicals to be detected even at this recovery. A likely route to improve temporal resolution and detect less abundant analytes is to use miniaturized analytical methods like capillary LC, CE, or droplet enzyme assays.[37,53–57] The sensitivity of such methods would allow good temporal resolution while preserving the advantages of better spatial resolution and lower tissue damage. The use of microfabricated probes may allow integration of other functionality such as electrodes for chemical or potential sensing, microfluidics for sample preparation (e.g. derivatization), or droplet formation for fraction collection at nanoliter scale. The probe may also be utilized for other applications that require continuous chemical sampling or delivery from microenvironments.

Supplementary Material

Refer to Web version on PubMed Central for supplementary material.

Acknowledgments

This work was supported by NIH R37 EB003320.

References

1. Tossman U, Ungerstedt U. Acta Physiol Scand. 1986; 128:9–14. [PubMed: 2876587]
2. Kehr J. J Neurosci Methods. 1993; 48:251–261. [PubMed: 8105153]
3. Nandi P, Lunte SM. Anal Chim Acta. 2009; 651:1–14. [PubMed: 19733728]
4. Darvesh AS, Carroll RT, Geldenhuys WJ, Gudelsky GA, Klein J, Meshul CK, Van der Schyf CJ. Exp Op Drug Disc. 2011; 6:109–127.
5. Watson CJ, Venton BJ, Kennedy RT. Anal Chem. 2006; 78:1391–1399. [PubMed: 16570388]
6. Yang CS, Tsai PJ, Chen WY, Liu L, Kuo JS. J Chromatogr B. 1995; 667:41–48.
7. Jansson P, Fowelin J, Smith U, Lonnroth P. Am J Physiol. 1988; 255:E218–E220. [PubMed: 3407771]
8. Fray A, Forsyth R, Boutelle M, Fillenz M. J Physiol. 1996; 496:49–57. [PubMed: 8910195]
9. Bungay PM, Newton-Vinson P, Isele W, Garris PA, Justice JB. J Neurochem. 2003; 86:932–946. [PubMed: 12887691]
10. Zahn JD, Trebotich D, Liepmann D. Biomed Microdevices. 2005; 7:59–69. [PubMed: 15834522]
11. Chen X, Prow TW, Crichton ML, Jenkins DW, Roberts MS, Frazer IH, Fernando GJ, Kendall MA. J Control Release. 2009; 139:212–220. [PubMed: 19577597]
12. Lee HJ, Son Y, Kim D, Kim YK, Choi N, Yoon ES, Cho IJ. Sens Actuator B-Chem. 2015; 209:413–422.
13. Chandrasekaran S, Brazzle JD, Frazier AB. J Microelectromech Syst. 2003; 12:281–288.
14. Lee JW, Park JH, Prausnitz MR. Biomaterials. 2008; 29:2113–2124. [PubMed: 18261792]
15. Verhoeven M, Bystrova S, Winnubst L, Qureshi H, De Gruijl TD, Scheper RJ, Luttge R. Microelectron Eng. 2012; 98:659–662.
16. Jina A, Tierney MJ, Tamada JA, McGill S, Desai S, Chua B, Chang A, Christiansen M. J Diabetes Sci Technol. 2014; 8:483–487. [PubMed: 24876610]
17. Ainla A, Jeffries GD, Brune R, Orwar O, Jesorka A. Lab Chip. 2012; 12:1255–1261. [PubMed: 22252460]
18. Li CG, Lee CY, Lee K, Jung H. Biomed Microdevices. 2013; 15:17–25. [PubMed: 22833155]
19. Lee WH, Slaney TR, Hower RW, Kennedy RT. Anal Chem. 2013; 85:3828–3831. [PubMed: 23547793]
20. Kotake, N.; Suzuki, T.; Mabuchi, K.; Takeuchi, S. Int. Conf. Miniaturized Syst. Chem. Life Sci., 12th; 2008; p. 1687-1689.
21. Metz, S.; Trautmann, C.; Bertsch, A.; Renaud, P. IEEE Int. Conf. Micro Electro Mech. Syst., 15th; 2002; IEEE; p. 81-84.
22. Desai TA, Hansford D, Ferrari M. J Membr Sci. 1999; 159:221–231.
23. Lebouitz, KS.; Mazaheri, A.; Howe, R.; Pisano, A. IEEE Int. Conf. Micro Electro Mech. Syst., 12th; 1999; IEEE; p. 470-475.
24. Chung HH, Chan CK, Khire TS, Marsh GA, Clark A, Waugh RE, McGrath JL. Lab Chip. 2014; 14:2456–2468. [PubMed: 24850320]
25. Leïchlé T, Bourrier D. Lab Chip. 2014
26. Striemer CC, Gaborski TR, McGrath JL, Fauchet PM. Nature. 2007; 445:749–753. [PubMed: 17301789]
27. Song S, Singh AK, Shepodd TJ, Kirby BJ. Anal Chem. 2004; 76:2367–2373. [PubMed: 15080749]
28. Song S, Singh AK, Kirby BJ. Anal Chem. 2004; 76:4589–4592. [PubMed: 15283607]
29. Hsieh YC, Zahn JD. J Diabetes Sci Technol. 2007; 1:375–383. [PubMed: 19885093]
30. Trautmann C, Brüchle W, Spohr R, Vetter J, Angert N. Nucl Instrum Methods Phys Res, Sect B. 1996; 111:70–74.
31. Poinern GEJ, Ali N, Fawcett D. Materials. 2011; 4:487–526.
32. Suh JS, Lee JS. Appl Phys Lett. 1999; 75:2047–2049.
33. Diggle JW, Downie TC, Goulding C. Chem Rev. 1969; 69:365–405.
34. Church WH, Justice JB Jr. Anal Chem. 1987; 59:712–716. [PubMed: 3565771]

35. Song P, Mabrouk OS, Hershey ND, Kennedy RT. Anal Chem. 2012; 84:412–419. [PubMed: 22118158]
36. Wu, S.; Bammatter, M-O.; Tang, W.; Auzelyte, V.; Zhang, H.; Brugger, J. IEEE Int. Conf. Nano/Micro Eng. Mol. Syst., 8th; 2013; IEEE; p. 986-989.
37. Slaney TR, Nie J, Hershey ND, Thwar PK, Linderman J, Burns MA, Kennedy RT. Anal Chem. 2011; 83:5207–5213. [PubMed: 21604670]
38. Wang M, Slaney T, Mabrouk O, Kennedy RT. J Neurosci Methods. 2010; 190:39–48. [PubMed: 20447417]
39. Song P, Hershey ND, Mabrouk OS, Slaney TR, Kennedy RT. Anal Chem. 2012; 84:4659–4664. [PubMed: 22616788]
40. Gerhardt G, Adams RN. Anal Chem. 1982; 54:2618–2620.
41. Popat KC, Mor G, Grimes CA, Desai TA. Langmuir. 2004; 20:8035–8041. [PubMed: 15350069]
42. Feichtner, F.; Schaupp, L.; Koehler, H. Devices for and methods of monitoring a parameter of a fluidic sample by microdialysis. US Patent. 8,535,537. Sep 17. 2013
43. Smith AD, Olson RJ, Justice JJB. J Neurosci Methods. 1992; 44:33–41. [PubMed: 1279321]
44. Herrera-Marschitz M, You ZB, Goiny M, Meana JJ, Silveira R, Godukhin OV, Chen Y, Espinoza S, Pettersson E, Loidl CF, et al. J Neurochem. 1996; 66:1726–1735. [PubMed: 8627331]
45. Lada MW, Kennedy RT. Anal Chem. 1996; 68:2790–2797. [PubMed: 8794915]
46. Fray AE, Boutelle M, Fillenz M. J Physiol. 1997; 504:721–726. [PubMed: 9401977]
47. Hashimoto A, Kanda J, Oka T. Brain Res Bull. 2000; 53:347–351. [PubMed: 11113591]
48. Kanamori K, Ross BD. J Neurochem. 2004; 90:203–210. [PubMed: 15198679]
49. Molchanova S, Oja SS, Saransaari P. Amino Acids. 2004; 27:261–268. [PubMed: 15549491]
50. Benveniste H, Hüttemeier PC. Prog Neurobiol. 1990; 35:195–215. [PubMed: 2236577]
51. Menacherry S, Hubert W, Justice JB Jr. Anal Chem. 1992; 64:577–583. [PubMed: 1580357]
52. Butcher SP, Fairbrother IS, Kelly JS, Arbuthnott GW. J Neurochem. 1988; 50:346–355. [PubMed: 2447237]
53. Tucci S, Rada P, Sepúlveda MJ, Hernandez L. J Chromatogr B. 1997; 694:343–349.
54. Boyd BW, Witowski SR, Kennedy RT. Anal Chem. 2000; 72:865–871. [PubMed: 10701275]
55. Song H, Chen DL, Ismagilov RF. Angew Chem, Int Ed. 2006; 45:7336–7356.
56. Shackman HM, Shou M, Cellar NA, Watson CJ, Kennedy RT. J Neurosci Methods. 2007; 159:86–92. [PubMed: 16876256]
57. Wang M, Hershey ND, Mabrouk OS, Kennedy RT. Anal Bioanal Chem. 2011; 400:2013–2023. [PubMed: 21465093]

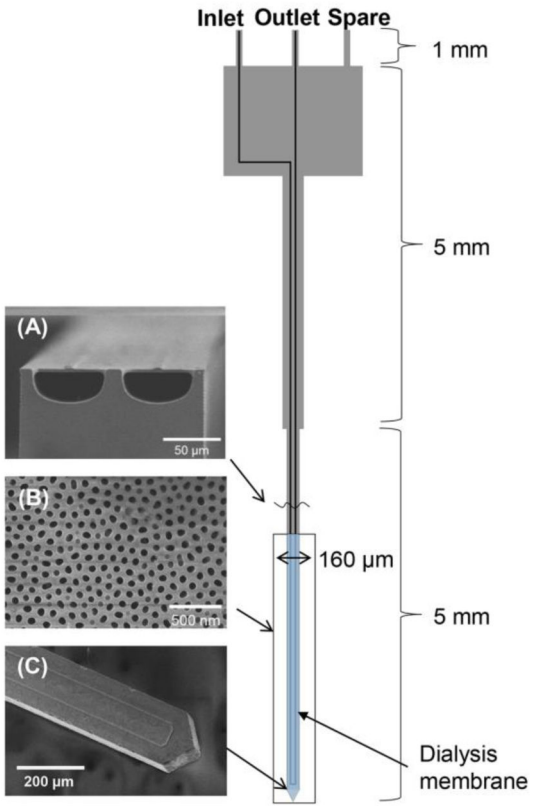

Figure 1.

Layout of microfabricated microdialysis probe. A probe has 3 ports including inlet, outlet, and spare for other potential uses (it was not used at this probe). (A) SEM image of cross-section of channels showing semicircular shape and thin polysilicon top layer. (B) SEM image of of AAO membrane over sampling area. (C) SEM image of sampling probe tip showing the channel pattern.

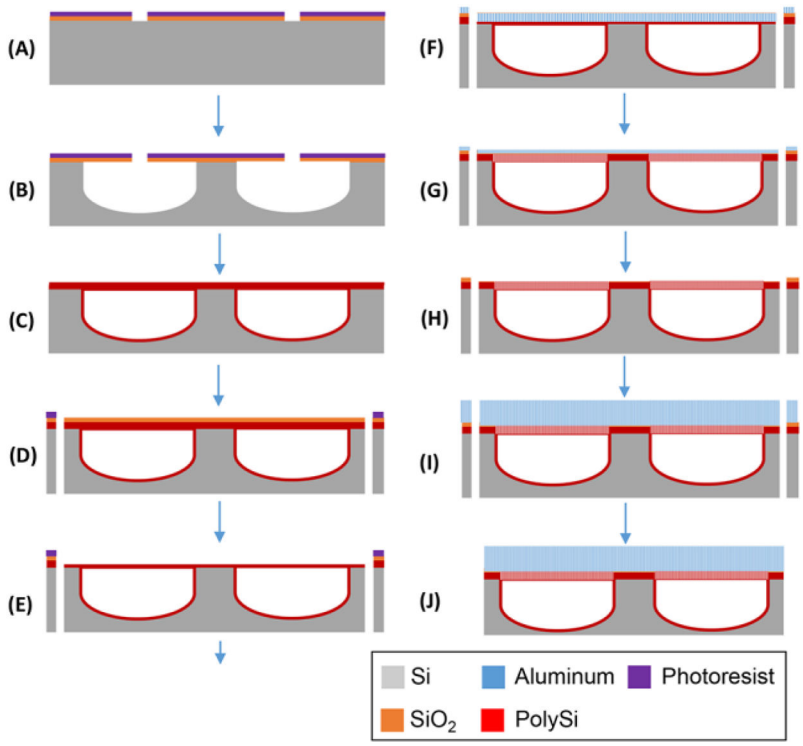

Figure 2.

Illustration of microfabrication process for microdialysis probe. The channel line was patterned on 2 μm thick SiO_2 grown Si wafer (A). Semicircular shaped channels with 60 μm wide and 30 μm high were etched by XeF_2 (B) and sealed with polysilicon (C). After 1 μm thick SiO_2 was deposited, probe shape was patterned and etched by DRIE (D). Sampling area at the tip of the probe was opened and etched by DRIE to be 2 μm thick layer (E). 400 nm Al layer was deposited and anodized electrochemically forming nanoporous AAO membrane (F). Polysilicon layer was etched through AAO membrane by DRIE (G) and 400 nm AAO membrane was removed (H). For physical strength of sampling area, 3 μm AAO membrane was fabricated by the deposition and electrochemical anodization of Al layer (I). Finally, thinned probes were released in hot water after backside etching (J).

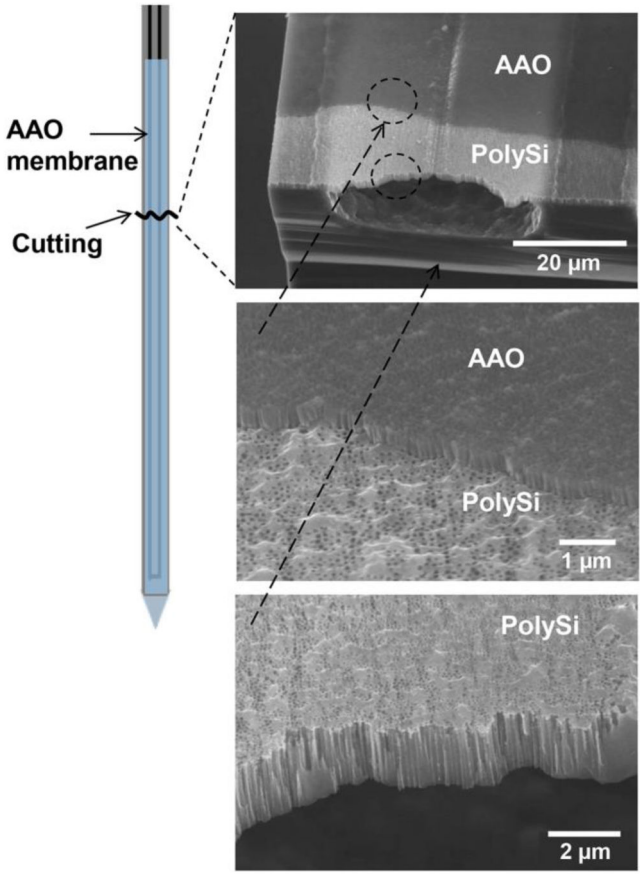

Figure 3.

Scanning electron micrographs of fabricated microchannels with pores. Drawing at left indicates where the probe sampling tip was broken to expose channels. Images show AAO and polysilicon membranes overlaid. Lowest image shows that pores go through the polysilicon base layer over the open channel.

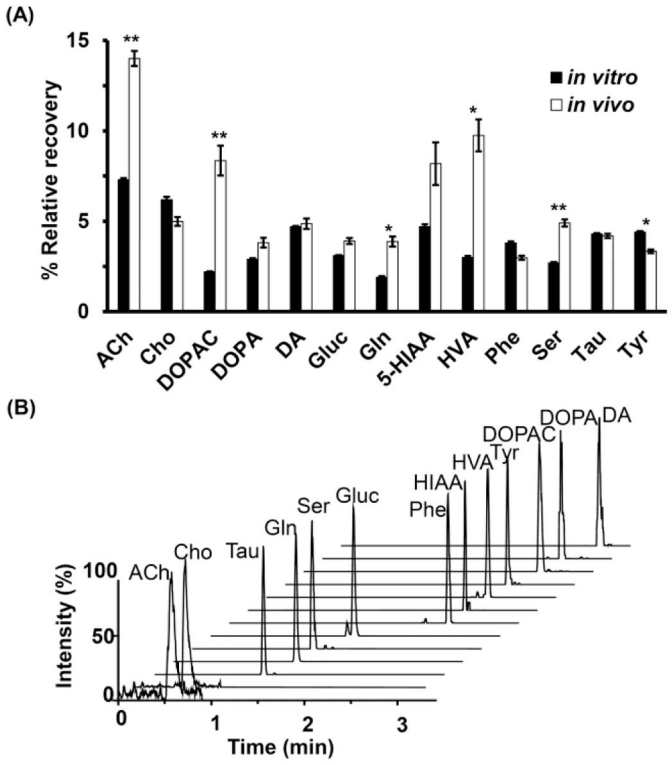

Figure 4.

(A) Comparison of relative recoveries of analytes between in vitro and in vivo experiments. The bar chart represents averaged relative recovery with SEM. * indicates different with $p < 0.05$, ** indicates $p < 0.001$ obtained by the two-tailed Student's t-test test. (B) Multiple reaction monitoring mass chromatograms of a representative fraction (1.5 μL) collected from the striatum of an anesthetized rat through the microfabricated probe. The chromatogram shows the trace for 13 detectable neurochemicals. Abbreviations used are: acetylcholine (ACh), choline (Cho), taurine (Tau), glutamine (Gln), serine (Ser), glucose (Gluc), phenylalanine (Phe), 5-hydroxyindoleacetic acid (5-HIAA), homovanillic acid (HVA), tyrosine (Tyr), 3,4-dihydroxyphenylacetic acid (DOPAC), 3,4-dihydroxyphenylalanine (DOPA), and dopamine (DA).

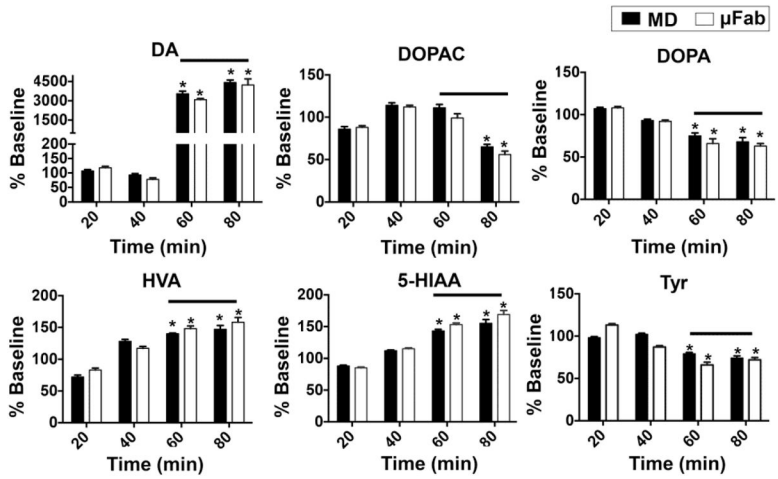

Figure 5.

Dual probe microdialysis of rat striatum showing effects of AMPH (5 mg/kg, IP) on DA release and other neurochemicals sampled by a concentric microdialysis probe (MD) and microfabricated probe (μFab). Both probe types have similar performance on response to dynamic *in vivo* chemical changes. Lines indicates when AMPH was present (fractions at 60 and 80 min). Data were converted to percent of baseline measurement to normalize pre-drug levels to 100 percent. Student's t-test indicates a significant change (*$p < 0.05$) between basal and post drug levels. Results are the mean ± SEM, n = 3 animals. For other measured neurochemicals, their post drug levels did not significantly change.

Table 1

Comparison basal extracellular concentration by the microfabricated probes, conventional probes with previous reports. The in vivo recovery for the microfabricated probes is estimated by finding the ratio between [μFab] and [MD]. All measurements are from sampling of the striatum of rats. Values given as mean ± SEM (n = 5 animals). In vivo recovery of μFab probe estimated by dividing μFab concentration by MD concentration, where recovery was estimated at 100%.

Analyte	Previously-reported concentration, μM (Anesthesia, Quantification method, Ref #)	Dialysate concentration, μM		Estimated in vivo recovery, %
		[MD]	[ufab]	
ACh	0.01 ± 0.003 (Ketamine, 20% in vitro recovery, 34)	0.032 ± 0.0045	0.0045 ± 0.00046	14 ± 0.4
Choline		11 ± 0.93	0.54 ± 0.022	5 ± 0.2
DOPAC	17.4 ± 2.6 (Awake, No-net-flux, 37)	8.9 ± 1.4	0.74 ± 0.084	8 ± 0.8
DOPA		0.15 ± 0.017	0.0056 ± 0.00041	4 ± 0.3
Dopamine	0.010 ± 0.0017 (Awake, No-net-flux, 37)	0.0067 ± 0.00062	0.00032 ± 0.000046	5 ± 0.3
Glucose	350 ± 20 (Awake, No-net-flux, 40)	1431 ± 82	56 ± 3.3	4 ± 0.2
GABA	0.12 ± 0.05 (Urethane, 20% in vitro recovery, 38)	0.78 ± 0.34	n.d.	-
Glutamine	385 ± 16 (Awake, No-net-flux, 42)	472 ± 24	18 ± 2.2	4 ± 0.3
Histamine		0.039 ± 0.016	n.d.	-
5-HIAA	3.5 ± 0.1 (Awake, Low-flow-rate, 37)	1.2 ± 0.13	0.095 ± 0.016	8 ± 1.2
HVA	17 ± 1.1 (Awake, Low-flow-rate, 37)	8.3 ± 1.1	0.81 ± 0.097	10 ± 0.9
3-MT		0.0069 ± 0.00046	n.d.	-
Phe	2 ± 0.2 (Chloral Hydrate, Low-flow-rate, 39)	7.5 ± 0.49	0.22 ± 0.012	3 ± 0.1
Serine	7 ± 0.5 (Awake, Corrected for in vitro recovery, 41)	36 ± 2.3	1.8 ± 0.12	5 ± 0.2
5-HT		0.019 ± 0.0042	n.d.	-
Taurine	25 ± 5.1 (Halothane, No-net-flux, 43)	60 ± 4.9	2.8 ± 0.21	4 ± 0.1
Tyrosine	3.3 ± 0.9 (Chloral Hydrate, Low-flow-rate, 39)	6.7 ± 0.33	0.22 ± 0.0011	3 ± 0.1